Patient Specific Identification of the Cardiac Driver Function in a Cardiovascular System Model

C.E. Hann[1], J. Revie[1], D. Stevenson[1], S. Heldmann[2], T. Desaive[3], C.F. Froissart[4], B. Lambermont[3], A. Ghuysen[3], P. Kolh[3], G.M. Shaw[5] and J.G. Chase[1]

[1] Department of Mechanical Engineering, Centre for Bio-Engineering, University of Canterbury, Christchurch, New Zealand
Email: Chris.Hann@canterbury.ac.nz

[2] Department of Mechanical Engineering, TU Darmstadt, Germany

[3] Hemodynamics Research Laboratory, University of Liege, Belgium

[4] Université de Technologie de Belfort-Montbéliard, France

[5] Department of Intensive Care, Christchurch Hospital, Christchurch, New Zealand

Abstract

The cardiac muscle activation or driver function, is a major determinant of cardiovascular dynamics, and is often approximated by the ratio of the left ventricle pressure to the left ventricle volume. In an intensive care unit, the left ventricle pressure is usually never measured, and the left ventricle volume is only measured occasionally by echocardiography, so is not available real-time. This paper develops a method for identifying the driver function based on correlates with geometrical features in the aortic pressure waveform. The method is included in an overall cardio-vascular modelling approach, and is clinically validated on a porcine model of pulmonary embolism. For validation a comparison is done between the optimized parameters for a baseline model, which uses the direct measurements of the left ventricle pressure and volume, and the optimized parameters from the approximated driver function. The parameters do not significantly change between the two approaches thus showing that the patient specific approach to identifying the driver function is valid, and has potential clinically.

1. Introduction

Inadequate diagnosis of cardiac disease and dysfunction is prevalent in critical care and is a significant cause of increased length of stay and death [1]. However, detection, diagnosis and treatment is very difficult, with clinicians confronted by a wealth of confusing, contradictory numerical data. The overall goal in this research is to put this clinical data into a readily understood physiological context for clinicians, by using computational models to uncover hidden dynamics and interactions to improve diagnosis.

In critical care, cardiac assessment commonly involves the analysis of changes in aortic pressure, cardiac output, ECG and gas exchange measurements relative to a normal or "average" patient. However complex interactions in these measurements can hide the underlying disease state, preventing proper treatment or detection [2]. Diagnosis is thus often based on potentially incomplete/flawed conceptual models and understanding of attending clinical staff. Hence, the primary problem is that the wealth of available data is not fully utilised to reveal these hidden dynamics and interactions.

This research shifts the focus to the fundamental dynamics of the cardiovascular system (CVS) using computer models and patient specific parameter identification to create patient specific models [3, 4]. The goal is to use the parameters in these models to directly represent the physiological status of the patient. From this computer aided physiological picture, clinical diagnosis is much easier as the data now fits clinical expectations and hidden physiological dynamics and interactions are exposed – a transformation from numerical data to physiology.

Recent work [5] has shown the potential for using simplified models that initially decouple the left and right sides of the circulation, to dramatically simplify parameter identification of a six chamber CVS model. A new concept of parameter identification was also introduced where changes in the parameters are treated as an actuation force into a feedback control system, where the reference output is taken to be steady state values of measured volume and pressure. The major advantage of the method is that

when it converges, it must be t the global minimum, so that the correct solution is always found. The method was validated on the left ventricle side for a fixed population driver function in simulation and on two time intervals of an animal experiment on one pig.

This paper first validates the methods on all five pigs of a porcine model of Pulmonary embolism [6], using a driver function which is derived directly from measured left ventricle pressure and volume waveforms. The results of this validation serve as a "gold standard" for comparison with another method that doesn't rely on the left ventricle pressure and volume waveforms. This method derives information from correlates of specific features in the driver functions and combines with the aortic pressure waveform and valve timing.

2. Methodology

2.1 Cardiac model

The cardiac model, is essentially a sub-model of a previously developed six chamber cardiac model [7, 8] with inertial effects and ventricular interaction. A schematic of the simplified model is shown in Figure 1. Note that this model can easily be extended to the right ventricle as well, but for this paper only the left side is considered. In Figure 1 the vena cava and pulmonary vein pressures are assumed constant and the model can be expressed in terms of differential equations defined:

$$\dot{V}_{lv} = H(Q_{mt})Q_{mt} - H(Q_{av})Q_{av} \tag{1}$$

$$\dot{P}_{ao} = E_{ao}H(Q_{av})Q_{av} - E_{ao}\left(\frac{P_{ao} - P_{vc}}{R_{sys}}\right) \tag{2}$$

$$Q_{mt} = \frac{P_{pu} - P_{lv}}{R_{mt}} \tag{3}$$

$$Q_{av} = \frac{P_{lv} - P_{ao}}{R_{av}} \tag{4}$$

$$P_{lv} = e(t)E_{es,lvf}V_{lv} + P_{th} \tag{5}$$

$$e(t) = \frac{P_{lv,measured}(t)}{V_{lv,measured}(t)} \tag{6}$$

where $e(t)$ in Equation (6) is derived from the measured left ventricle pressure and volume waveforms. Note that the thoracic pressure P_{th} in Equation (5) is set to 0 in this case, as the animal experiments [6] are open heart.
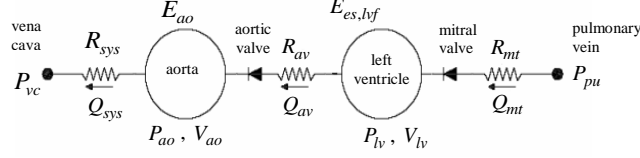

Figure 1: The left ventricle-systemic system simplified model

2.2 Parameter identification

The parameter identification method is adapted slightly from [5] so is reproduced here. The unknown patient specific parameters denoted X, that are optimized for the left ventricle model of Equations (1)-(6), are defined:

$$X \equiv \left\{ P_{pu}, E_{es,lvf}, E_{ao}, R_{mt}, R_{av}, R_{sys} \right\} \tag{7}$$

The parameter P_{vc} in Equation (2) is assumed known, since it would be found from either identifying the right ventricle system, or by direct measurement of the central venous pressure, which is common in an intensive care unit.

There are 6 unknown parameters in Equation (7) to be identified in the model of Figure 1. Therefore, the measured maximum/minimum left ventricle volume and aortic pressure can only uniquely identify 4 of these parameters. However, the time of the mitral valve closure $t_{mt,close}$ corresponds to the end of the atrial contraction which can be detected by the end of the P wave on an electrocardiogram (ECG) [9, 10]. In addition, the beginning of ejection can be found from the time of minimum aortic pressure t_{min} [9, 10]. The difference between these time values is known as the isovolumetric contraction (ivc) [9, 10] and is defined:

$$\Delta T_{ivc} = t_{min} - t_{mt} \tag{8}$$

Increasing the parameter R_{mt} in the model by a factor of two has the effect of reducing the period of isovolumetric contraction by a factor close to two, and vice versa. Therefore, an approximation to R_{mt} is defined:

$$R_{mt,approx} = \frac{\Delta T_{ivc,approx}}{\Delta T_{ivc,true}} R_{mt,old} \qquad (9)$$

Hence, if $R_{mt,old}$ in Equation (9) is larger than the true value, $\Delta T_{ivc,approx}$ will be smaller than $\Delta T_{ivc,true}$, which will have the effect of reducing $R_{mt,approx}$ and will bring it closer to the true value.

A further important feature available is the maximum gradient or inflection point in the ascending aortic pressure wave. The parameter which has a significant effect on the maximum aortic pressure gradient is the resistance in the aortic valve R_{av}. Define:

$$\alpha(R_{av}) = \frac{P_{ao,true}(t_{inflect}) - P_{ao,true}(t_{min})}{P_{ao,approx}(t_{inflect}) - P_{ao,approx}(t_{min})} \qquad (10)$$

where $P_{ao,approx}$ and $P_{ao,true}$ are the simulated and "measured" aortic pressures, t_{min} is the time of minimum aortic pressure and $t_{inflect}$ is the time of maximum aortic pressure gradient. Equation (10) is an approximation to the ratio of the maximum gradients of $P_{ao,approx}$ to $P_{ao,true}$ and is used to avoid having to differentiate the aortic pressure which may be noisy. Simulation has shown that the variable α in Equation (10), changes inversely proportional to R_{av} with all other parameters held at their nominal values. Specifically, if R_{av} increases by a factor of 2, with all other parameters fixed, α approximately reduces by a factor of 2, with a order of magnitude less effect on the maximum and minimum volumes/pressures. This result motivates an approximation to R_{av}:

$$R_{av,approx} = \frac{P_{ao,approx}(t_{inflect}) - P_{ao,approx}(t_{min})}{P_{ao,true}(t_{inflect}) - P_{ao,true}(t_{min})} R_{av,old} \qquad (11)$$

To obtain the highest accuracy and robustness, the solution proposed, is to first ensure that the maximum/minimum simulated volumes and aortic pressures are precisely matched to the measured values for given initial (but essentially arbitrary)

estimates of R_{mt} and R_{av}. At the end of this optimization, R_{mt} and R_{av} are updated using Equations (9) and (11).

Simulation has shown that increasing the parameter $E_{es,lvf}$, by a factor of 2 decreases the mean volume. On the other hand, increasing the parameters for E_{ao}, R_{sys} and P_{pu} proportionally increase the pulse pressure difference, the mean aortic pressure and the stroke volume. These results motivate the following definitions:

$$E_{es,lvf,approx} = \left(\frac{V_{lv,min,approx} + V_{lv,max,approx}}{V_{lv,min,true} + V_{lv,max,true}} \right) E_{es,lvf,old} \tag{12}$$

$$P_{pu,approx} = \left(\frac{SV_{true}}{SV_{approx}} \right) P_{pu,old} \tag{13}$$

$$E_{ao,approx} = \left(\frac{PP_{true}}{PP_{approx}} \right) E_{ao,old} \tag{14}$$

$$R_{sys,approx} = \left(\frac{P_{ao,max,true} + P_{ao,min,true}}{P_{ao,max,approx} + P_{ao,min,approx}} \right) R_{sys,old} \tag{15}$$

Note that another reason for separating the optimization of R_{mt} and R_{av} in Equations (9) and (11) with the parameters in Equations (12)-(15), is that physiologically, the valve resistances do not change unless stenosis occurs. Stenosis usually takes months or years to develop so it would not be expected for these resistances to change significantly during a patient's stay in the ICU, which is typically 3-7 days. However, to account for the possible effect of varying degrees of stenosis, the resistances R_{mt} and R_{av} are optimized separately between patients, but for an individual patient are held constant over time. In contrast, the other parameters in Equations (12)-(15) can change on the order of minutes to hours depending on the disease state or drugs given, so they are optimized regularly on the time scale of minutes to hours.

The tests for the parameter identification method are done on five pigs from the porcine model of pulmonary embolism [6]. For the animal experiments, the measured data is from catheters [6] and the data set used is defined:

$$data \equiv mean\ V_{lv}, SV, PP, mean\ P_{ao}, P_{ao}(t), t_{d2} \tag{16}$$

where:

$$\text{mean } V_{lv} = \frac{V_{lv,max} + V_{lv,min}}{2}, \quad SV = V_{lv,max} - V_{lv,min},$$

$$PP = P_{ao,max} - P_{ao,min}, \quad \text{mean } P_{ao} = \frac{P_{ao,max} + P_{ao,min}}{2}, \tag{17}$$

$$\Delta T_{ivc} \text{(from Equation (8))}$$

The overall parameter identification method is summarized in Figure 2.

Step1 Choose arbitrary set of input parameters including R_{mt} and R_{av}.

Step2 Simulate model of Equations (1)-(6) .

Step3 Compute approximations to $E_{es,lvf}$, P_{pu}, E_{ao} and R_{sys} from Equations (12)-(15).

Step4 Simulate model Equations (1)-(6).

Step5 If the maximum volumes and aortic pressures are matched within a given tolerance go to Step6, otherwise go back to Step3.

Step6 Compute R_{mt} and R_{av} from Equations (9) and (11). If they have changed by less than 1% go to Step7 otherwise go back to Step3.

Step7 Output final solution and identified parameters.

Figure 2: Parameter identification algorithm for Figure 1

Notice that the updates in Equations (9)-(15), are similar to proportional feedback control. That is, these parameters can be considered to be the actuation force that controls the reference output, which is the data in Equation (16). The only difference is that instead of applying a force proportional to the difference between the reference and actual output, the force is proportional to the ratio of the reference to actual output.

2.3 Driver function identification

The driver function or time varying elastance consists of four main features as shown in Figure 3. The ascending inflection point corresponds to the beginning of ejection,

the "shoulder" is the second slower ejection, the peak is the repolarization of the ventricle or T wave on ECG, and the descending inflection point is the end of ejection or beginning of filling [6, 10].
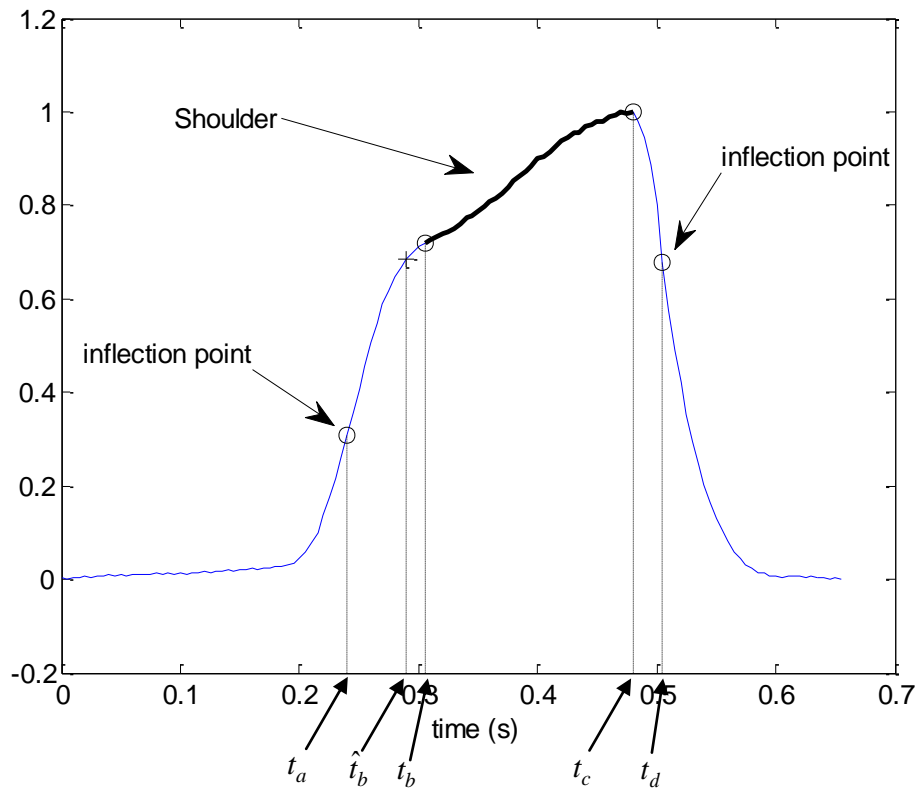

Figure 3: Overall shape of driver function with main features labelled including time points.

The shape of the driver function in Figure 3 can change significantly, due to a change in heart rate or contractility, but the overall shape will still contain the main features in Figure 3. To track the driver function directly over time using Equation (6) requires continuous measurements of left ventricle pressure and volume which are not usually available in an ICU.

However, a significant amount of information on the driver function can be derived from the continuous aortic pressure waveform [10]:

$$t_a \simeq \hat{t}_a = \text{time of minimum aortic pressure}$$

$$t_b \simeq \hat{t}_b + 0.015, \ \hat{t}_b = \text{time of ascending inflection point of aortic pressure}$$

$$t_c \simeq \hat{t}_c = \text{time of maximum aortic pressure}$$

$$t_d \simeq \hat{t}_d = \text{time of diacrotic notch}$$

$$\tag{18}$$

Note that the value of $\hat{t}_b$ always occurs before the curves moves on to the shoulder, so the constant 0.015 is chosen empirically to ensure the shoulder is reached. This value was found to be reasonably constant over all pigs, and was sufficient to determine correlations.

The remaining key unknowns in Figure 3 are:

$$e'_{t_a} \equiv \text{slope of ascending inflection point at } t = t_a$$

$$e_{t_a} \equiv \text{height of } e(t) \text{ at } t = t_a$$

$$e_{t_b} \equiv \text{height of shoulder } e(t) \text{ at } t = t_b \tag{19}$$

$$e'_{t_d} \equiv \text{slope of descending inflection point at } t = t_d$$

$$e_{t_d} \equiv \text{height of } e(t) \text{ at } t = t_d$$

The unknowns in Equation (19) can be correlated to features in the aortic pressure waveform. For example, Figure 4 plots e'_{t_a} versus $\dfrac{P'_{ao,ta}}{period}$ for all pigs, where the period is used to normalize out the heart rate, and to improve the correlation. The values of $P'_{ao,ta}$ and $P'_{ao,td}$ correspond to the maximum and minimum gradients in the aortic pressure. The r value in Figure 4 is 0.98 showing a very strong correlation.
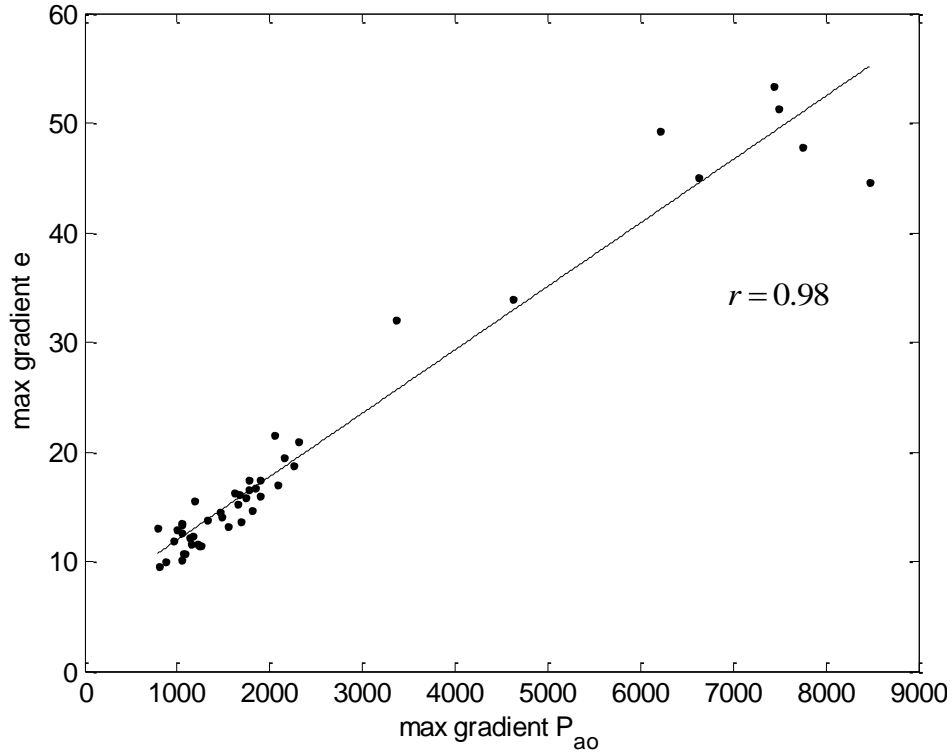
Figure 4: Correlation between maximum gradient in e and maximum gradient in P_{ao}

All correlations are summarized:

$$e'_{t_a} = 0.0055\frac{P'_{ao,ta}}{period} + 6.36, \quad r = 0.98$$

$$e_{t_a} = 103.88e'_{t_a} - 24.43, \quad r = 0.86$$

$$e_{t_b} = 0.0075e'_{t_a} + 0.61, \quad r = 0.86 \tag{20}$$

$$e'_{t_d} = 0.0051\frac{P'_{ao,td}}{period} - 17.82, \quad r = 0.58$$

$$e_{t_d} = 10.6l8\frac{P'_{ao,td}}{period} - 29.77, \quad r = 0.28$$

where the lower correlations in Equation (20) are due to the values of e'_{t_d} and e_{t_d} being relatively constant over all pigs. The correlations in Equation (20) and the time points in Equations (21) can be used to reconstruct the required features of the driver function in Figure 3. The function used for the approximation is defined:

$$\hat{e}_{approx} = E_1(t), \quad 0 < t \le t_b$$

$$= E_1(t_b) + \left(\frac{E_2(t_c) - E_1(t_b)}{t_c - t_b} \right)(t - t_b), \quad t_b \le t \le t_c \tag{22}$$

$$= E_2(t), \quad t_c \le t \le period$$

$$E_i(t) = a_i e^{-b_i(t - c_i)^2}, \quad i = 1, 2 \tag{23}$$

For $E_1(t)$, it is assumed that $c_1 = t_b$. In other words, the turning point of $E_1(t)$ is assumed to be at the beginning of the shoulder. However, the approximation for t_b in Equation (18) is only an average over all pigs and can change. Therefore, t_b is assumed to be an unknown. Thus, the parameters a_1, b_1 and c_1 can be determined analytically:

$$a_1 = e_{t_b}, \quad b_1 = -\frac{1}{4} \frac{e_{t_a}'^2}{\ln\left(\frac{e_{t_a}}{e_{t_b}}\right) e_{t_a}^2}, \quad t_b = \frac{t_a e_{t_a}' - 2\ln\left(\frac{e_{t_a}}{e_{t_b}}\right) e_{t_a}}{e_{t_a}'}, \quad c_1 = t_b \tag{24}$$

where:

$$E_1(t_a) = e_{t_a}, \quad E_1(t_b) = e_{t_b}$$
$$E_1'(t_a) = e_{t_a}' \tag{25}$$

Note that the function $\hat{e}_{approx}$ in Equation (26) does not explicitly enforce an inflection point at t_a even though the true driver function has an inflection point here. It turns out, that in all cases, the time of the inflection point of $\hat{e}_{approx}$ coincides very closely with t_a, typically within 0.005 and at most 0.01 seconds. However, this result is not critical, as the driver function is always very close to a straight line around the inflection point, so the maximum slope of the driver function is always closely captured by $\hat{e}_{approx}$. Replacing t_a, t_b with t_d, t_c and E_1 with E_2 in Equations (27)-(28) gives a similar method for finding the parameters a_2, b_2, c_2.

3. Results

To validate the methods presented, data from a data from a porcine pulmonary embolism experiment is used. The data is obtained from the Hemodynamics Research Laboratory, University of Liege, Belgium. In the experiments, a pig is injected with autologous blood clots every two hours to simulate pulmonary embolism [6]. The parameter identification method of Figure 2 is applied to this pig data using the measured parameters of Equation (29), for both the measured driver function of Equation (6) and the identified driver function from Figure 4.

For each pig, R_{mt} and R_{av} are initially identified separately for every time period and then the average of all the R_{mt} and R_{av} values are taken to be the final identified values. This approach ensures that the iso-volumetric time of Equation (30) and the ascending aortic pressure slope are matched on average throughout the experiment, and enforces the physiological constraint that R_{mt} and R_{av} are constant over time for each pig. The final values of R_{mt} and R_{av} are then fixed in step 6 of Figure 2, and the remaining parameters in Equation (31) are re-identified.

3.1 Measured driver function

The maximum and minimum left ventricle volumes and aortic pressures are matched very accurately over all pigs with a maximum error of 5.2% in the volumes and 0.2% in the pressures. All model responses errors are summarized in Table 1. The mean of the identified parameters of four time periods for one of the pigs (pig 8) is shown in Table 2. The contractility $E_{es,lvf}$ increases and the pulmonary vein pressure increases slowly as well. The systemic resistance R_{sys} also increases a little then drops, though this effect is not so pronounced in pig 8. These results are consistent with physiological expected changes in pulmonary embolism.

	Max/Min V_{lv}	Max/Min P_{ao}	**Max P_{lv}**	**Max P_{ao} slope**	ΔT_{ivc}
Max % error	5.2	0.2	4.9	24.3	11.2

Table 1: Model response errors over all pigs with measured driver function

Time interval	**30-60 (mins)**	**90-150**	**180-240**	**255-270**
E_{lv} (Hg/ml)	1.85	1.89	2.01	2.75
R_{sys} (mmHg s/ml)	2.20	2.38	2.22	2.20
E_{ao} (Hg/ml)	2.23	2.40	2.68	3.19
P_{pu} (mmHg)	4.64	4.74	5.37	5.85
R_{av} (mmHg s/ml)	0.037	0.037	0.037	0.037
R_{mt} (mmHg s/ml)	0.031	0.031	0.031	0.031

Table 2: Average identified parameters for pig 8.

3.2 Identified driver function

The method of Equations (32)-(33) is now applied to identify the driver functions in the pig data. Figure 5 shows an example of the identified versus measured driver functions for four time periods in pig 8.
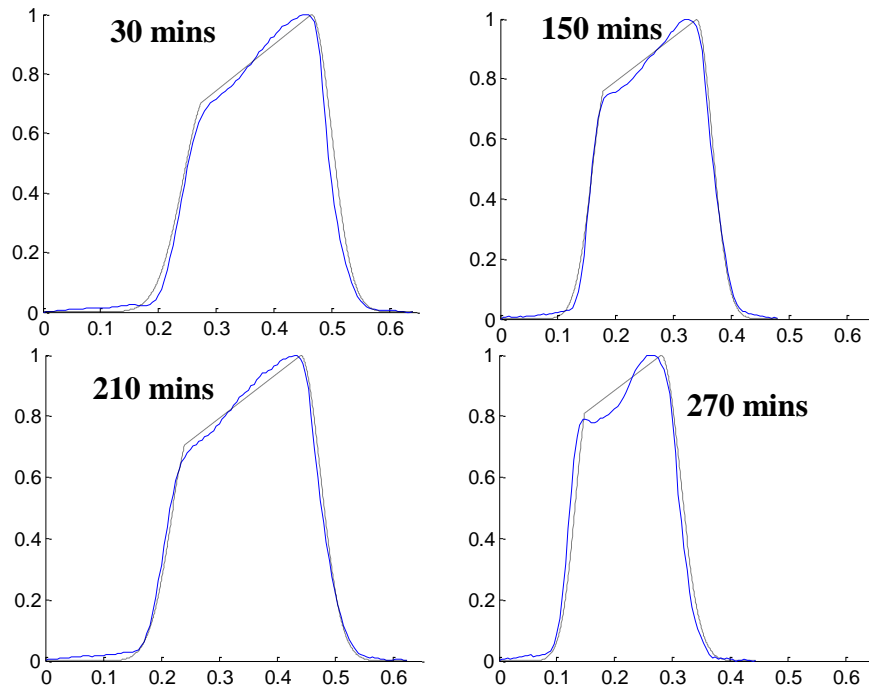
Figure 4: Comparing the measured driver function to approximated driver function over 4 time intervals in pig 8.

The mean absolute error in the approximation of the driver function compared to the true over all pigs was 0.15. However, importantly as shown in Figure 2, the upward slope and downward slope are accurately captured. The results of the parameter identification method of Figure 2 with the identified driver function are compared to the results for the measured driver function in Table 3. The mean values of $E_{es,lvf}$, R_{sys} and E_{ao} vary from 0.5-5.1 %, and the error in P_{pu} is around 10%. However, note that the absolute difference in the approximated values of P_{pu} are typically within 1 mmHg of the baseline, which is more than adequate clinically. The resistances R_{av} and R_{mt} are less accurate, but the model outputs are relatively insensitive to changes in R_{av} so the values of 18.6-30.1% are quite good and are expected. It is also known [5] that errors in mitral valve timing and isovolumetric time can have a significant effect on R_{mt}, and overestimates of R_{mt} give underestimates of P_{pu}. Mitral and aortic stenosis are typically simulated as 300-500% changes so 20-30% is more than enough to capture this disease state, but more clinical validation is needed to

understand to what accuracy these parameters are needed for adequate diagnosis. Figure 5 gives an example of comparing the modelled pressure volume curve and aortic pressure based on the approximated driver function, to the measured curves, showing a close match. Model response errors are also very similar to the results for the measured driver function in Table 1 so are not shown.

	$E_{es,lvf}$	R_{sys}	E_{ao}	P_{pu}	R_{av}	R_{mt}
Pig 1	2.2	0.9	5.1	11.2	27.2	29.6
Pig 2	1.4	0.8	4.6	14.1	30.1	34.1
Pig 7	0.7	0.5	3.4	9.8	24.3	18.7
Pig 8	0.8	0.7	3.7	13.2	20.5	25.2
Pig 9	0.8	1.1	2.9	10.4	18.6	20.4
Overall	1.2	0.8	3.9	11.7	24.1	25.6

4. Discussion and conclusion

A method for identifying a time varying patient specific cardiac driver function was developed. The method was validated for the left ventricle on a porcine model of pulmonary embolism. For comparison, a baseline model was established by matching data using this measured driver function. The method used for matching was adapted from previous work but with the addition of enforcing a constraint on the resistances R_{av} and R_{mt} that they remain constant for a given pig, but can vary between pigs. This approach allows for the possibility of diagnosing acute mitral or aortic stenosis. The main physiological trends of pulmonary embolism were captured including an increase in contractility and systemic resistance as well as a slower overall increase in pulmonary vein pressure. All measured data was accurately captured including the left ventricle pressure which was not used in the identification.

Very accurate matches were obtained to a measured driver function based on the ratio of the left ventricle pressure to the left ventricle volume waveforms. Identification

was achieved using geometrical correlations between the aortic pressure and measured driver function with two exponential base driver functions. These curves represented the ascending and descending parts, and a linear model represented the shoulder of the driver function. In all cases the ascending maximum and descending minimum gradients were accurately captured as well as the height of the shoulder which physiologically corresponds to the twisting of the ventricle in the slower part of ejection.

Furthermore, the method accurately captured significant changes in the driver function as a result of increasing heart rate. The results suggest that a robust method for calculating the driver function based only on the aortic pressure waveform is potentially available, but needs further validation on other disease states and humans. Importantly, when comparing the parameters identified from the approximated driver function with the parameters from the measured driver function, there were no significant changes. This results shows that removing the left ventricle pressure and volume profiles does not lose accuracy in the diagnostic power of the model. The results give confidence that a physiologically accurate model can be derived given data typically available in an ICU.

5. References

[1]   D. C. Angus, W. T. Linde-Zwirble, J. Lidicker, G. Clermont, J. Carcillo, and M. R. Pinsky, "Epidemiology of severe sepsis in the United States: analysis of incidence, outcome, and associated costs of care," *Critical care medicine,* vol. 29, pp. 1303-10, Jul 2001.

[2]   K. Dickstein, "Diagnosis and assessment of the heart failure patient: the cornerstone of effective management," *European journal of heart failure,* vol. 7, pp. 303-8, Mar 16 2005.

[3]   C. Starfinger, J. G. Chase, C. E. Hann, G. M. Shaw, B. Lambermont, A. Ghuysen, P. Kolh, P. Dauby, and T. Desaive, "Model-based identification and diagnosis of a porcine model of induced endotoxic shock with hemofiltration," *Math Biosci,* vol. 216(2), pp. 132-139, 2008.

[4]   C. Starfinger, C. E. Hann, J. G. Chase, T. Desaive, A. Ghuysen, and G. M. Shaw, "Model-based cardiac diagnosis of pulmonary embolism," *Comput Methods Programs Biomed,* vol. 87(1), pp. 46--60, Jul 2007.

[5]   C. E. Hann, J. G. Chase, T. Desaive, C. F. Froissart, J. Revie, D. Stevenson, B. Lambermont, A. Ghuysen, P. Kolh, and G. M. Shaw, "Unique Parameter

Identification for Cardiac diagnosis in Critical Care using Minimal Data Sets," *Comput Methods Programs Biomed, in press,* 2009.

[6]   A. Ghuysen, B. Lambermont, P. Kolh, V. Tchana-Sato, D. Magis, P. Gerard, M. Mommens, N. Janssen, T. Desaive, and V. D'Orio, "Alteration of Right Ventricular-Pulmonary Vascular Coupling in a Porcine Model of Progressive Pressure Overloading," *Shock,* vol. 29(2), pp. 197-204, 2007.

[7]   C. E. Hann, J. G. Chase, and G. M. Shaw, "Efficient implementation of non-linear valve law and ventricular interaction dynamics in the minimal cardiac model," *Comput Methods Programs Biomed,* vol. 80(1), pp. 65--74, Oct 2005.

[8]   B. W. Smith, J. G. Chase, R. I. Nokes, G. M. Shaw, and G. Wake, "Minimal haemodynamic system model including ventricular interaction and valve dynamics," *Medical Engineering & Physics,* vol. 26(2), pp. 131-139, 2004.

[9]   A. C. Guyton and J. E. Hall, *Textbook of medical physiology*, 10th ed.: W.B. Saunders Company, Philadelphia, 2000.

[10]   R. E. Klabunde, *Cardiovascular Physiology Concepts*: Lippincott Williams and Wilkins, 2004.